

Cosmological populations of massive black hole binaries

Alberto Sesana¹§, Marta Volonteri²§, Emanuele Berti²§ for the new LISA Taskforce

¹ Albert Einstein Institute, Am Mühlenberg 1 D-14476 Golm, Germany

² Department of Astronomy, University of Michigan, Ann Arbor, MI 48109

³ Department of Physics and Astronomy, The University of Mississippi, University, MS 38677-1848, USA

Abstract. This document contains the detailed description of the material included in this massive black hole binary population directory. We summarize the relevant physics of the models giving the appropriate references, and describe the content of each file column by column. We also include some sample figure to illustrate the relevant features of the binary populations. We provide 5 catalogues of binary mergers. The first four catalogues are meant to be used for Model Selection (we follow the naming convention used by the first LISAPE taskforce), the fifth catalogue is to be used for the Horizon estimation.

- SE.** Small seeds, Efficient spin evolution. Model VHM, coherent accretion (aligned spins), gas driven dynamics (for eccentricity evolution);
- SC.** Small seeds, Chaotic spin evolution. Model VHM, chaotic accretion (randomly oriented spins), star driven dynamics (for eccentricity evolution);
- LE.** Large seeds, Efficient spin evolution. Model BVR, coherent accretion (aligned spins), gas driven dynamics (for eccentricity evolution);
- LC.** Large seeds, Chaotic spin evolution. Model BVR, chaotic accretion (randomly oriented spins), star driven dynamics (for eccentricity evolution).
- HOR:** an ‘average’ model, constructed by summing up the distributions $d^3N_i/dM_z dq dz$ (being M_z the total redshifted binary mass and $q = M_2/M_1 < 1$ the binary mass ratio) and dividing by four. This model should be used for the ‘horizon determination’ of the new gravitational wave detector.

§ email: alberto.sesana@aei.mpg.de

§ email: martav@umich.edu

§ email: berti@phy.olemiss.edu

1. Massive black hole formation and evolution models

One of the targets of the new-LISA Parameter Estimation Taskforce is to assess the capabilities of a descoped LISA to detect supermassive black holes and measure their parameters. The cosmological evolution of massive black holes can be determined by merger tree simulations, following the merger history of dark matter halos and of the associated black holes by cosmological Monte Carlo realizations of the merger hierarchy from early times until the present in a Λ CDM cosmology with $H_0 = 70 \text{ km s}^{-1} \text{ Mpc}^{-1}$, $\Omega_M = 0.3$ and $\Omega_\Lambda = 0.7$. Merger tree simulations were used to produce ascii files listing the masses, redshifts and spins of merging black holes. The sample binaries used in the Taskforce are selected to assess the capabilities of LISA, not to allow for a reliable (and statistically significant) analysis of the black hole population.

Two important sources of uncertainty in merger tree models of black hole formation are (i) the formation mechanism and mass of the first "seed" black holes, and (ii) the details of how accretion causes black holes to grow in time (see [1] for more details). To bracket these uncertainties we focused on four representative models of massive black hole formation.

- **Seed masses.** As a representative model with "light" black hole seeds we considered the Volonteri-Haardt-Madau ([2], henceforth VHM) scenario, where light seed black holes of $m_{\text{seed}} \sim \text{few times } 100 M_\odot$ are produced as remnants of metal-free stars at redshift $z \gtrsim 20$. Koushiappas, Bullock and Dekel suggested an alternative scenario where "heavy" seeds with $m_{\text{seed}} \sim 10^5 M_\odot$ are formed as the end-product of dynamical instabilities arising in massive gaseous protogalactic disks in the redshift range $10 \lesssim z \lesssim 15$ [3]. To allow for the possibility of heavy seeds, we considered a variant of this scenario proposed by Begelman, Volonteri and Rees ([4], henceforth BVR). Both models (VHM and BVR) can reproduce the AGN optical luminosity function in the redshift range $1 \lesssim z \lesssim 6$, but they result in very different coalescence rates of massive black hole binaries and hence in different gravitational wave backgrounds [1].

- **Spin evolution.** To bracket uncertainties in the evolution the black holes' *spin magnitude* due to accretion, we considered two different accretion models. We adopted either a "coherent accretion" scenario, where accretion of material with constant angular momentum axis rapidly spins up the holes [5, 6], or a "chaotic accretion" scenario [7], where accretion always proceeds via very small and short episodes (caused by fragmentation of the accretion disc where it becomes self-gravitating). Since counter-rotating material spins black holes down more efficiently than co-rotating material spins them up, and it is quite unlikely for mergers to produce rapidly spinning holes, this scenario implies that black hole spins are typically rather small [8]. The accretion prescription also leaves an imprint on the *mass growth* of black holes, and therefore on the masses of the two components at merger. The models assume that the mass-to-energy conversion efficiency, ϵ , depends on black hole spin only, so the two models predict different average efficiencies of $\sim 20\%$ and $\sim 10\%$ respectively. The mass-to-energy conversion directly affects mass growth, with high efficiency implying slow growth, since for a black hole accreting at the Eddington rate, the black hole mass increases with time as

$$M(t) = M(0) \exp\left(\frac{1 - \epsilon}{\epsilon} \frac{t}{t_{\text{Edd}}}\right) \quad (1)$$

where $t_{\text{Edd}} = 0.45 \text{ Gyr}$. Therefore black holes in the SC and LC models are on average more massive than in the SE and LE models at a given cosmic time. The "coherent"

versus “chaotic” models thus allow us to study how different growth rates affect LISA observations. Finally, the assumed accretion prescription is likely to have an important effect on *spin alignment*. In gas-rich environments, the torque exerted by the gas is efficient in producing alignment of the black hole angular momenta with the (dominant) angular momentum of the circumbinary accretion disk (which has the same direction of the orbital angular momentum of the binary), as suggested in [9], and found in detailed SPH simulations by Dotti and collaborators [10] (see Ref. [8] for more details). If accretion proceeds in a chaotic fashion, there is no privileged direction for the spins of the black holes, and they can be assumed to be isotropically distributed.

- **Eccentricity.** We also include eccentricity in our models. Exactly circular massive black hole binaries are unlikely to exist in nature. Both gas driven and stellar driven binary evolution have been found to excite the eccentricity of the binary [11, 12, 13]. In the coherent accretion scenario, the massive circumbinary disk is likely to be also the dominant source of secular binary evolution. In this case, the binary is expected to achieve a limiting eccentricity of ~ 0.6 [12], which is maintained through the inspiral until efficient gravitational wave emission takes over. The situation is less clear in the chaotic scenario. For the sake of comparison between different eccentricity evolution models, in this latter case we assume that the binary evolution is driven by stars. We employ the hybrid model proposed by [13] in which the binary evolves via scattering of bound and unbound stars in the galactic bulge. The process usually results in fairly high eccentricities. When the gravitational wave shrinking timescale is shorter than the gas/star driven binary migration, the binary decouples by its environment and circularizes. However, a significant amount of eccentricity can be retained at the moment it enters the frequency band relevant to gravitational wave observations, as shown in figure 3. It is worth mentioning that eccentricity evolution is implemented *a posteriori* on each individual binary, and it is not self consistently implemented in the merger trees.

1.1. Details of the merger tree implementation

For each formation scenario, we usually have $N_{\text{tree}} \sim 10$ different “merger trees” [14]. A merger tree traces the merger history that leads to a $z = 0$ galaxy in a hierarchical cosmology. Each merger tree is characterized by a different mass of the parent halo at $z = 0$ and by a different Press-Schechter weight $W_{\text{PS}}^{(k)}$ ($k = 1, \dots, N_{\text{tree}}$) [15, 16], which is used to scale the results to the (comoving) number density of sources. Furthermore, each merger tree has a different number $N_{\text{real}}^{(k)}$ of realizations to take into account cosmic variance. Typically, large-mass halos have a smaller Press-Schechter weight (inherent in the adopted cosmological model) and a smaller number of realizations (due to computational burden).

For each tree k we have a list of black hole masses, spins and redshifts. All quantities in these files are measured in the source frame, at variance with the convention used in the Mock LISA Data Challenge (recall that $M = (1 + z)M_{\text{source}}$). Each row in the list corresponds to “branches” of the tree where a merger event occurs. Including all merger trees and all realizations of each merger tree, in a typical model such as VHM we have at least $\sim 5 \times 10^4$ merging events.

The number of events at a given redshift z per comoving volume is

$$N_{\text{com}}(z) = \sum_{k=1}^{N_{\text{tree}}} \sum_{j=1}^{N_{\text{mergers}}^{(k)}} \frac{W_{\text{PS}}^{(k)}}{N_{\text{real}}^{(k)}}, \quad (2)$$

The rate of potentially observable events at $z = 0$ (note that no SNR cut has been performed in equation 2) per unit time and redshift is then given by Eq. (11) of Ref. [17] (see also [18]):

$$\frac{d^2 N}{dz dt} = 4\pi c N_{\text{com}}(z) [D_a(1+z)]^2 = 4\pi c N_{\text{com}}(z) D_c^2, \quad (3)$$

where D_c is the comoving distance and D_a is the angular diameter distance, both evaluated at redshift z .

2. Detailed content of the files

To summarize, we have four black hole formation and evolution models, and we provide 5 catalogues of binary mergers. The first four catalogues are meant to be used for Model Selection (we follow the naming convention used by the first LISAPE taskforce), the fifth catalogue is to be used for the Horizon estimation. The models are labeled with different IDs (SE, SC, LE, LC, HOR), and each file name contains the ID of the reference models. The IDs are:

- **SE.** Small seeds, Efficient spin evolution. Model VHM, coherent accretion (aligned spins), gas driven dynamics (for eccentricity evolution);
- **SC.** Small seeds, Chaotic spin evolution. Model VHM, chaotic accretion (randomly oriented spins), star driven dynamics (for eccentricity evolution);
- **LE.** Large seeds, Efficient spin evolution. Model BVR, coherent accretion (aligned spins), gas driven dynamics (for eccentricity evolution);
- **LC.** Large seeds, Chaotic spin evolution. Model BVR, chaotic accretion (randomly oriented spins), star driven dynamics (for eccentricity evolution).
- **HOR:** an ‘average’ model, constructed by summing up the distributions $d^3 N_i / dM_z dq dz$ (being M_z the total redshifted binary mass and $q = M_2/M_1 < 1$ the binary mass ratio) and dividing by four. This model should be used for the ‘horizon determination’ of the new gravitational wave detector.

2.1. Directory merger-trees

Here we collect the raw (before Press & Schechter weighting and comoving volume integration) merger tree outputs. There are 48 files **spins-merge-*-model***: 12 files (101-to-112) for each of the four models (SE-to-LC). Each file contains several realizations (20 for files 1-to-10, 10 for file 11, 5 for file 12) of a halo of a specific mass. The columns are as follows:

- 1-redshift
- 2-3-nevermind
- 4- M_1 (in the source frame)
- 5-mass ratio, $q = M_2/M_1 \leq 1$
- 6-normalized spin magnitude of black hole 1, a_1
- 7-normalized spin magnitude of black hole 2, a_2

- 8-nevermind

The file **PS-J.dat** contains the twelve Press & Schechter weights (1-to-12 from the top to the bottom).

2.2. Directory distributions

Here we collect the relevant binned distributions of each model. The files **model*-DNzmq.OUT** contain the trivariate distributions $\Delta^3 N / (\Delta z \Delta M_z \Delta q)$ evaluated on a grid in (z, M_z, q) . If desired, any new Montecarlo realization of the black hole population can be extracted directly from these files. In all the files located in this directory, grids are as follow:

- The z interval $[0, 20]$ is divided in 20 intervals. of width $\Delta z = 1$ in the range.
- The $\log M_z$ interval $[1, 11]$ is divided in 40 equally spaced log bins.
- The $\log q$ interval $[-5, 0]$ is divided in 30 equally spaced log bins.
- The a interval $[0, 0.998]$ is divided in 100 equally spaced bins.

The columns are as follows.

(i) Files **model*-DNzmq.OUT**

- column 1-lower bound of the z bin
- column 2-lower bound of the M_z bin
- column 3-lower bound of the q bin
- column 4- $\Delta^3 N / (\Delta z \Delta M_z \Delta q)$, events predicted by the models

These distributions are normalized so that the sum over all the bins is equal to $N_{3\text{yr}}$ (i.e. $\sum_{\Delta z} \sum_{\Delta M_z} \sum_{\Delta q} \Delta^3 N / (\Delta z \Delta M_z \Delta q) = N_{3\text{yr}}$), i.e. the total number of events predicted by the model in a three year observation (240 for model SE; 227 for model SC; 72 for model LE; 67 for model LC; 151 for model HOR).

(ii) Files **model*-DNz.OUT**:

- column 1-lower bound of the z bin
- column 2-upper bound of the z bin
- column 3- $\Delta N / \Delta z$, total events predicted by the model

(iii) Files **model*-DNm.OUT**:

- column 1-lower bound of the log of the M_z bin
- column 2-upper bound of the log of the M_z bin
- column 3- $\Delta N / \Delta M_z$, events predicted by the models

(iv) Files **model*-DNq.OUT**:

- column 1-lower bound of the log of the q bin
- column 2-upper bound of the log of the q bin
- column 3- $\Delta N / \Delta q$, events predicted by the models

(v) Files **model*-DNa1a2.OUT**:

- column 1-lower bound of the spin bin
- column 2-upper bound of the spin bin
- column 3- $\Delta N / \Delta a_1$, for the primary black hole
- column 4- $\Delta N / \Delta a_2$, for the secondary black hole

Files (ii-v) contain differential distributions normalized to $\sum_{\Delta X} (\Delta N / \Delta X) \Delta X = N_{3\text{yr}}$, where X is either z , M_z , q , a_1 , a_2 . These distributions are useful to compare marginal distributions as shown in figures 2 and 3.

N.B. There is no spin distribution for model HOR. For horizon studies, we suggest to assume two extreme cases for the spins:

- 1-no spin
- 2- $a_1 = a_2 = 0.9$, aligned to the binary angular momentum.

2.3. Directory Montecarlo catalogues

In this directory we place the files **model*-MCEvents.OUT**, containing the Montecarlo catalogues to be used for parameter estimation, model selection study, etc. There are 10 realizations for models SE, SC, LE,LC and 100 realizations for model HOR, to provide better statistics for horizon determination studies, if desired. A file containing only the first realization of the HOR model (model-HOR-MCEvents-test.OUT, 140 coalescences) is provided as a reference for all groups to run the basic horizon studies.

The number of sources in each realization is drawn by a Poissonian distribution with a mean given by $N_{3\text{yr}}$ (240 for model SE; 227 for model SC; 72 for model LE; 67 for model LC; 151 for model HOR). Columns are as follows:

- column 1-realization ID
- column 2-source ID
- column 3-source redshift
- column 4- M_1 (restframe) in solar masses
- column 5-mass ratio q
- column 6-ecliptic longitude, ϕ_s (random in the interval $[0, 2\pi]$)
- column 7-ecliptic latitude, θ_s (in the interval $[-\pi/2, \pi/2]$, sampled with probability $\cos(\theta_s + \pi/2)$)
- column 8-azimuthal direction of the binary orbital angular momentum L , ϕ_L (random in the interval $[0, 2\pi]$)
- column 9-polar direction of the binary orbital angular momentum L , θ_L (in the interval $[0, \pi]$, sampled with probability $\cos\theta_L$)
- column 10-initial phase, ϕ (random in the interval $[0, 2\pi]$)
- column 11-coalescence time t_c in seconds (random in the interval $[0, 3\text{yr}]$)
- column 12-magnitude of spin 1
- column 13-magnitude of spin 2
- column 14-polar direction of spin 1, θ_{a_1} (in the interval $[0, \pi]$, sampled with probability $\cos\theta_{a_1}$ for chaotic models; = 0 for coherent models)
- column 15-polar direction of spin 2, θ_{a_2} (in the interval $[0, \pi]$, sampled with probability $\cos\theta_{a_2}$ for chaotic models (SC,LC); = 0 for coherent models (SE, LE))
- column 16-azimuthal direction of of spin 1, ϕ_{a_1} (random in the interval $[0, 2\pi]$ for chaotic models (SC,LC); = 0 for coherent models (SE,LE))
- column 17-6-azimuthal direction of of spin 2, ϕ_{a_2} (random in the interval $[0, 2\pi]$ for chaotic models (SC,LC); = 0 for coherent models (SE,LE))
- column 18-azimuthal direction of the binary pericenter, γ (random in the interval $[0, 2\pi]$)
- column 19-residual eccentricity at an *observed* gravitational wave frequency of 10^{-4} Hz. Where the gravitational wave frequency is intended to be the frequency of the second harmonic (i.e. twice the orbital *redshifted* frequency)

The binary lies in the $x - y$ plane of the (x, y, z) reference frame centered in its center of mass, with orbital angular momentum L initially pointing in the z direction. The angles defining the individual binary spins $(\theta_{a_1}, \phi_{a_1}, \theta_{a_2}, \phi_{a_2})$ the binary phase (ϕ) and the direction of the initial binary periastron (γ) are measured in this frame, with azimuthal angles measured counterclockwise starting from the x axis. The x axis points from the source toward the Earth. The angles defining the direction of the binary angular momentum L (θ_L, ϕ_L) , i.e. the orientation of the binary plane) and the sky location (θ_s, ϕ_s) , are measured in the ecliptic frame (x_e, y_e, z_e) . [Stas and Antoine will provide a script to transform the angles in a standard reference frame.]

N.B. For model HOR, only the first 11 columns are present. We consider the binaries to be circular in this case. As stated before, for horizon studies, we suggest to assume two extreme cases of (i) non spinning binaries, and (ii) binaries with $a_1 = a_2 = 0.9$, aligned to the binary angular momentum.

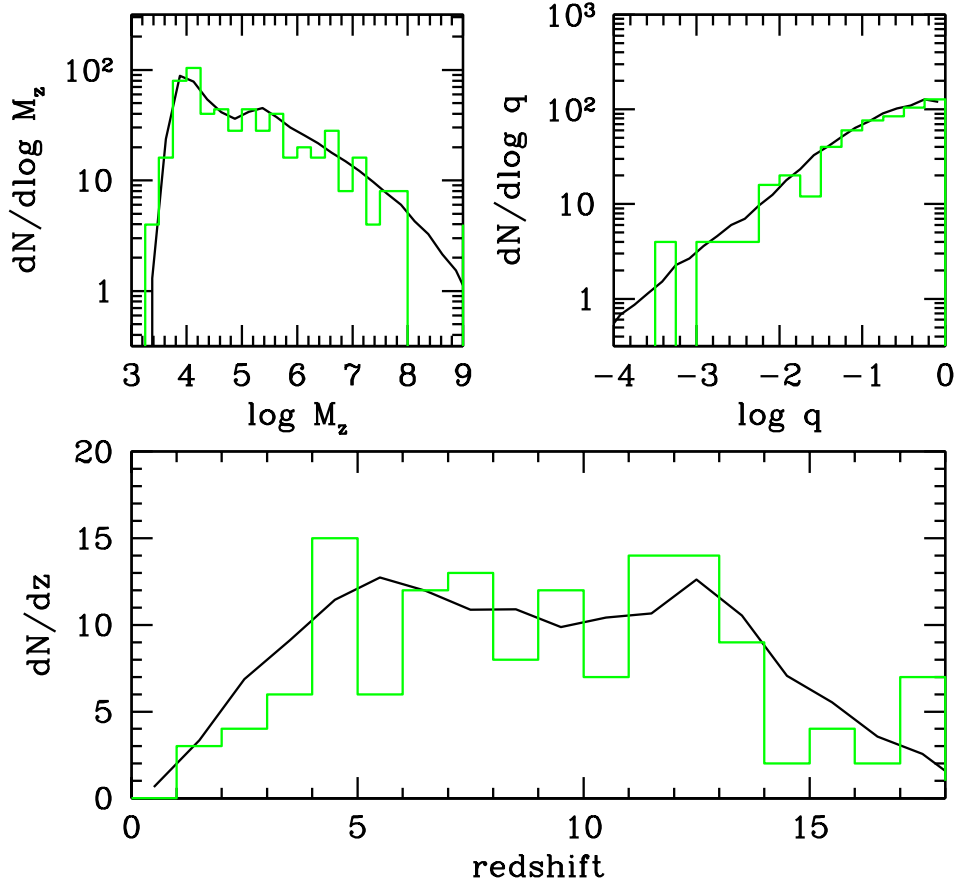


Figure 1. Example of marginalized dN/dM_z (upper left panel), dN/dq (upper right panel) and dN/dz (lower panel) distributions for model HOR. In each panel, the black lines are the marginalized distributions contained in the files located in the directory 'distributions'. The green histograms are the distributions obtained by realization 1 in the file model-HOR-MCevents.OUT in the 'montecarlo-catalogues' directory.

- [1] A. Sesana, M. Volonteri and F. Haardt, *Mon. Not. Roy. Astron. Soc.* **377**, 1711 (2007) [arXiv:astro-ph/0701556].
- [2] M. Volonteri, F. Haardt and P. Madau, *Astrophys. J.* **582**, 559 (2003) [arXiv:astro-ph/0207276].
- [3] S. M. Koushiappas, J. S. Bullock and A. Dekel, *Mon. Not. Roy. Astron. Soc.* **354**, 292 (2004) [arXiv:astro-ph/0311487].
- [4] M. C. Begelman, M. Volonteri and M. J. Rees, *Mon. Not. Roy. Astron. Soc.* **370**, 289 (2006) [arXiv:astro-ph/0602363].
- [5] J. M. Bardeen, *Nature* **226**, 64 (1970).
- [6] K. S. Thorne, *Astrophys. J.* **191**, 507 (1974).
- [7] A. R. King and J. E. Pringle, *Mon. Not. Roy. Astron. Soc. Lett.* **373**, L93 (2006) [arXiv:astro-ph/0609598].
- [8] E. Berti and M. Volonteri, *Astrophys. J.* **684**, 822 (2008) [arXiv:0802.0025].
- [9] T. Bogdanovic, C. S. Reynolds and M. C. Miller, *Astrophys. J. Lett.* **661**, 147 (2007)

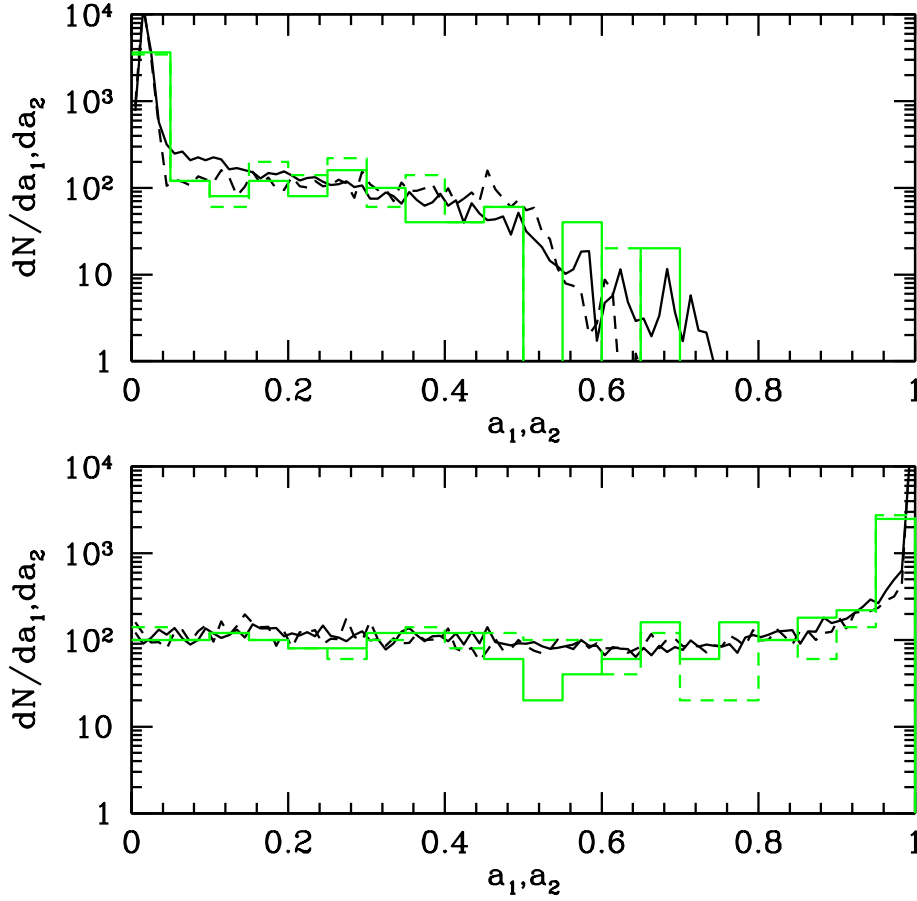


Figure 2. Example of marginalized spin distributions dN/da_1 (solid lines) and dN/da_2 (dashed lines) for models SE (VHM coherent, lower panel) and SC (VHM chaotic, upper panel). Histograms are the distributions obtained by realization 1 in the file model-SC-MCevents.OUT (upper panel) and model-SE-MCevents.OUT (lower panel) in the 'montecarlo-catalogues' directory.

- [arXiv:astro-ph/0703054].
- [10] M. Dotti, M. Volonteri, A. Perego, M. Colpi, M. Ruzkowski, F. Haardt, *Mon. Not. Roy. Astron. Soc.* **402**, 628 (2010).
- [11] J. Cuadra, P. J. Armitage, R. D. Alexander, M. C. Begelman, *Mon. Not. Roy. Astron. Soc.* **393**, 1423 (2009).
- [12] C. Roedig, M. Dotti, A. Sesana, J. Cuadra, M. Colpi, to appear in *Mon. Not. Roy. Astron. Soc.* (2011) [arXiv:astro-ph/1104.3868].
- [13] A. Sesana, *Astrophys. J.* **719**, 851 (2010)
- [14] C. G. Lacey and S. Cole, *Mon. Not. Roy. Astron. Soc.* **262**, 627 (1993).
- [15] W. H. Press and P. Schechter, *Astrophys. J.* **187**, 425 (1974).
- [16] R. K. Sheth and G. Tormen, *Mon. Not. Roy. Astron. Soc.* **329**, 61 (2002) [arXiv:astro-ph/0105113].
- [17] M. G. Haehnelt, *Mon. Not. Roy. Astron. Soc.* **269**, 199 (1994) [arXiv:astro-ph/9405032].
- [18] K. Menou, Z. Haiman and V. K. Narayanan, *Astrophys. J.* **558**, 535 (2001) [arXiv:astro-

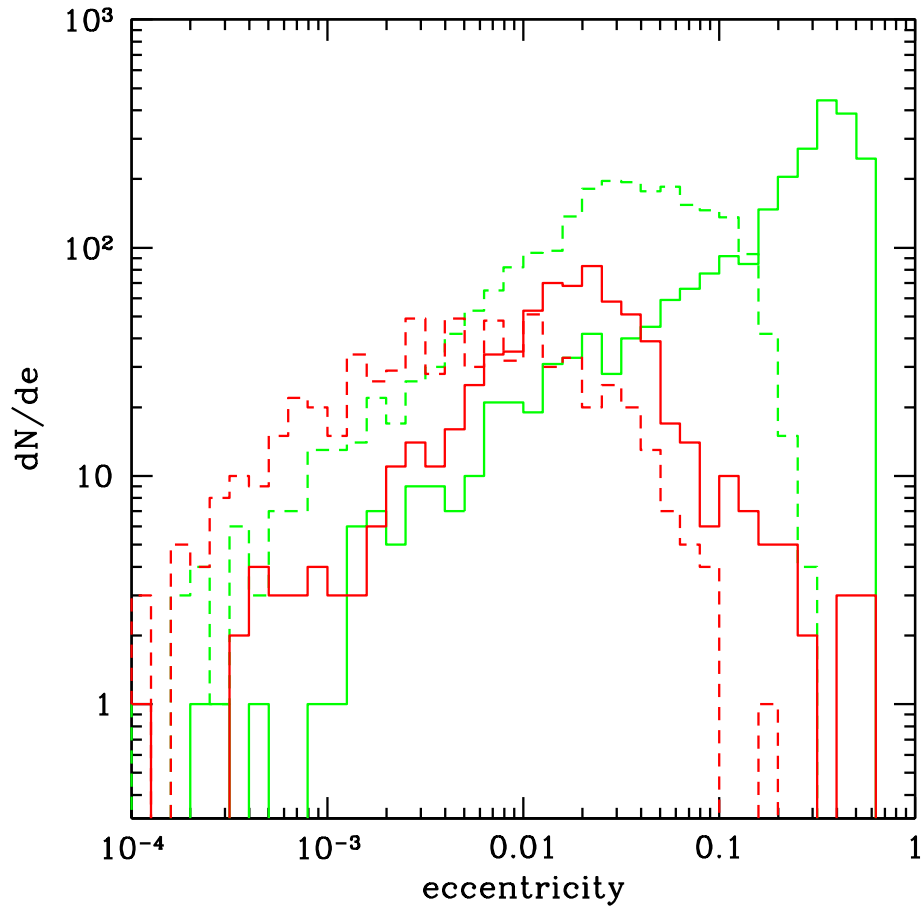


Figure 3. Eccentricity distributions at *observed* gravitational wave frequency of 10^{-4} Hz for model SE (VHM coherent, solid green histogram), SC (VHM chaotic, dashed green histogram), LE (BVR coherent, solid red histogram), LC (BVR chaotic, dashed red histogram). Coherent models are evolved via gas dynamics, whereas star driven dynamics is assumed for the chaotic models. The distributions are obtained by averaging over the 10 Montecarlo realizations contained in the respective model*-MCEvents.OUT files in the 'montecarlo-catalogues' directory.